Combining and Comparing Morphometric Shape Descriptors with a Molecular Phylogeny: The Case of Fruit Type Evolution in Bornean *Lithocarpus* (Fagaceae)

CHARLES H. CANNON[1,2,3] AND PAUL S. MANOS[2]

[1]*Institute for Biodiversity and Environmental Conservation, University of Malaysia, Sarawak, Kota Samarahan, Sarawak, Malaysia 94300*
[2]*Department of Biology, Duke University, Durham, North Carolina 27708, USA*

Abstract.—Fruit type in the genus *Lithocarpus* (Fagaceae) includes both classic oak acorns and novel modifications. Bornean taxa with modified fruits can be separated into two sections (*Synaedrys* and *Lithocarpus*) based on subtle shape differences. By following strict criteria for homology and representation, this variation in shape can be captured and the sections distinguished by using elliptic Fourier or eigenshape analysis. Phenograms of fruit shape, constructed by using restricted maximum likelihood techniques and these morphometric descriptors, were incorporated into combined and comparative analyses with molecular sequence data from the internal transcribed spacer (ITS) region of the nuclear rDNA, using branch-weighted matrix representation. The combined analysis strongly suggested independent derivation of the novel fruit type in the two sections from different acorn-like ancestors, while the comparative analysis indicated frequent decoupling between the molecular and morphological changes as inferred at well-supported nodes. The acorn fruit type has undergone little modification between ingroup and outgroup, despite large molecular distance. Greater morphological than molecular change was inferred at critical transitions between acorn and novel fruit types, particularly for section *Lithocarpus*. The combination of these two different types of data improved our understanding of the macroevolution of fruit type in this difficult group, and the comparative analysis highlighted the significant incongruities in evolutionary pattern between the two datasets. [Branch length estimates; continuous characters; eigenshape; enclosed receptacle; Fourier; matrix representation.]

Taxonomic classification of infrageneric groups and species within the genus *Lithocarpus* Bl. (Fagaceae) is based largely on morphological features of the mature fruit and its subtending cupule (Barnett, 1944; Camus, 1952–1954; Liao, 1969; Soepadmo, 1968a; Soepadmo, 1968b; Soepadmo, 1970; Soepadmo, 1972; Julia and Soepadmo, 1998; Cannon and Manos, 2000), because little variation in sterile and floral morphology exists at even the subfamily level (Forman, 1966a; Forman, 1966b). Traditional cladistic analysis of the genus is further complicated by the narrow range of variation and large amount of parallel evolution in cupule features (Soepadmo, 1970; Soepadmo, 1972; Jenkins, 1993). This difficult situation requires innovative and objective methods to properly investigate the evolutionary dynamics of fruit type.

Outline analysis (Ferson et al., 1985) of radial dissections of mature fruit has revealed informative variation in the internal structure of the fruit wall and receptacle at many taxonomic levels, including individual populations (Cannon and Manos, 2000). Two main fruit types exist in the genus: 1) the "acorn" which is almost identical to the *Quercus* acorn (Soepadmo, 1968b) and 2) the enclosed receptacle or "ER" fruit which is marked by the seed being enclosed within a woody receptacle (Fig. 1). In this plane of dissection, several homologous points are consistently present in all fruit and outline shape of the various fruit layers are separated by smooth distinct boundaries. The creation of discrete character states to capture subtle shape variation between and within these two fruit types is difficult and simply separating the fruit types into two states, "acorn vs. ER," would ignore a great deal of information. Therefore, we explored the use of morphometric techniques for shape analysis and developed a method for incorporating these continuous descriptors into phylogenetic and evolutionary analyses.

Although many types of morphometric shape descriptors exist, two main techniques are suitable for structures with few landmarks and an outline shape described by a closed smooth contour: elliptic Fourier (Kuhl and Giardina, 1982; Kincaid and Schneider,
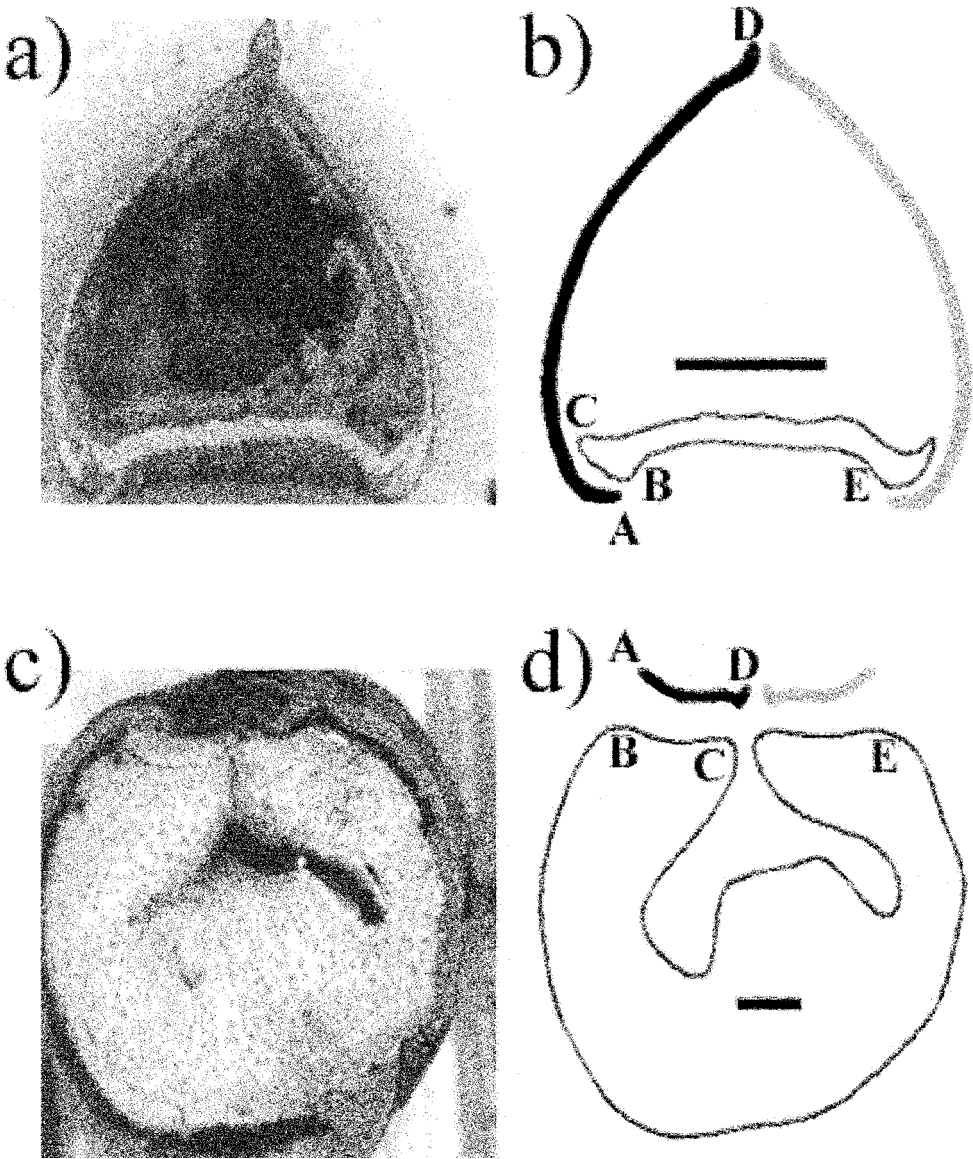

FIGURE 1.   Homology in the two main fruit types of genus *Lithocarpus* (Fagaceae). (a–b) "acorn" fruit—(*L. conocarpus*; M. Leighton T12607) where the seed has developed above the flattened receptacle, expanding the fruit wall. Points B&E mark the perimeter of the concave to flat abscission layer between cupule and fruit receptacle. Points A&D are the proximal and distal edges of the exocarp, which forms a hard cone over the seed. Points B&C measure the thickness of the outer edge of the receptacle. Points A&B measure the distance between the proximal ends of exocarp and receptacle, separated by the layers of the pericarp. (c–d) "enclosed receptacle" or ER fruit—(*L. kalkmannii*; W. Meijer SAN42460), where the seed remains embedded in the receptacle and the vestigial exocarp forms a small flat apical layer. Scale bar = 5 mm. Due to the fruit's radial symmetry, only one side of the exocarp (black) was used in the analysis, the other side is shown in dark gray. All images were oriented horizontally using point A on both the black and grey exocarp outlines.

1983; Rohlf and Archie, 1984; Rohlf, 1990; Crampton, 1995; McLellan and Endler, 1998) and eigenshape analysis (Lohmann and Schweitzer, 1990; MacLeod, 1999). These descriptors have been used in both phenetic and evolutionary studies (Mou and Stoermer, 1992; Ray, 1992; Lestrel et al., 1993; Ferrario et al., 1996; Renaud et al., 1996; Laurie et al., 1997; Richards and Esteves, 1997; Cronier et al., 1998; Kincaid et al., 1998; Mancuso, 1999; McLellan, 2000; Torres et al., 2000) and only minor differences

exist in their mathematical derivation (Rohlf, 1986).

To address major evolutionary questions about fruit type in *Lithocarpus*, we combined and compared fruit shape variation, using both morphometric techniques, with molecular sequences from the internal transcribed spacer (ITS) regions of the nuclear ribosomal DNA. The main questions addressed by this study were:

1. Are the chosen outline shape descriptors informative at this taxonomic level and how do they differ?
2. Given informative variation, how can these descriptors be incorporated into a combined phylogenetic analysis with molecular data?
3. Given the best estimates of phylogenetic relationship, what can be inferred about morphometric and molecular divergence patterns?

MATERIALS AND METHODS

Fruit Tissue Types and Homology

Several authors have described structural morphology of the mature cupule and fruit in *Lithocarpus* (Camus, 1948; Liao, 1969; Soepadmo, 1970; Kaul, 1987; Kaul, 1989). The two tissue types under study here form the bulk of the mature fruit wall. The laminate exocarp forms the outer layer of the fruit or pericarpium (Roth, 1977; Spjut, 1994) and consists of a single layer of columnar cells, harder and more brittle than underlying tissues. In the majority of the species of Fagaceae, the exocarp encloses most of the fruit and the abscission scar formed between the receptacle and the cupule is small and concave (Fig. 1). In radial section, its boundaries are clearly different from other fruit tissues.

The portion of the fruit receptacle internal to the abscission layer between the seed and the cupule forms the second tissue type. It closes the bottom of the carpels and its edge lies near the exocarp at its basal fringe (Fig. 1). The mature morphology of this woody layer varies among species, particularly in the degree to which it encloses the developed seed. Its boundaries are distinct from other internal fruit tissues because of its granular texture arising from extensive vascularization (Langdon, 1939). The sometimes numerous

pericarp layers are mostly laminate, creating multiple layers separated by dense tomentum.

After numerous dissections, only four landmarks could be consistently recognized in all specimens: the A) basal and D) apical edges of the exocarp and the C) inner and B) outer perimeters of the fruit receptacle (Fig. 1). Other landmarks were not consistently present in all taxa. The number and density of the pericarp layers were highly variable and their shape at maturity was largely dependent on the exocarp and receptacle shapes, therefore these layers were not included in the analysis.

Samples

Radial sections of 192 mature nuts were made from 21 *Lithocarpus*, two *Quercus*, and one *Chrysolepis* species (see Appendix A). Representatives from the latter two genera were chosen as outgroups. Potentially more closely related species of the genus *Castanopsis* were excluded from the analysis because many of the modifications in fruit type examined in this study are also found in this genus (Camus, 1952–1954; Forman, 1966b; Soepadmo, 1968a), thus requiring a separate analysis to assess evolutionary pattern and polarity in the outgroup. *Chrysolepis chrysophylla* (Douglas ex Hooker) Hjelmquist represents a relictual genus in North America of the largely paleotropical Castaneoideae subfamily (Nixon, 1997). It possesses a complex and unique cupule type but fruit wall structure is similar to that found in *Lithocarpus*. Secondly, the genus *Quercus* possesses a fruit type almost identical to the *Lithocarpus* "acorn" type and therefore these taxa can be used to root both the molecular and morphological reconstructions.

Although the twenty-one species of *Lithocarpus* included in this study represent less than half of the total diversity found on the island of Borneo, the selected taxa encompass all of the morphological variation found in fruit type. No Bornean taxa possessing the ER fruit type are absent from the analysis. Molecular sequence data were obtained for ten additional taxa, all possessing the acorn fruit type, but preliminary analysis indicated little change in resolution or topology of relationships pertaining to the evolution of the ER fruit type. Because of limited morphological samples for these taxa and a desire to limit

the overall complexity of this analysis, an exemplar approach seemed advantageous for the remaining acorn-fruited taxa.

Radial symmetry of mature nuts allowed the stylar column to define the plane of dissection for all specimens. Because of the range in size and thickness of the fruit wall, dissecting equipment ranged from an electric band saw to a razor blade. Images of the dissected nuts were captured in various ways, primarily with a Burle electronic analog camera mounted with a Nikkor 55 mm lens. Additional images were captured with an Olympus D-400 digital camera. Images were checked for planar distortion with a 1 cm test grid to ensure shape fidelity, as some lenses at certain magnifications can warp images at their margins. Outlines of the two tissue types were traced both manually and digitally. The proximal ends of the exocarp were aligned with the horizontal coordinate system to standardize image orientation (Point A, Fig. 1). Maintaining proper orientation of fruit structures to the central axis, along the plane of dissection, was important for consistent data capture. The basal and apical ends of exocarp outlines were further aligned with the horizontal plane, to standardize for rotation. The angle of rotation from the horizontal of the original outline was measured for each sample and means were calculated for each species. Mean angle of rotation was used as an additional observation in the exocarp data matrix.

Coordinate lists were obtained in either Image 1 or tpsDIG 1.20 (Rohlf, 1998b) and exported into EFAWIN (Isaev and Denisova, 1995) to perform the elliptic Fourier (EF) transformation. Coefficients were made invariant to size and location, as performed by EFAWIN (Rohlf and Archie, 1984), but not to rotation or starting point, both of which were standardized before transformation. Twenty harmonics were collected for each specimen. Outlines produced by these coefficients were reproduced in Mathematica 4.0 (Wolfram, 1998) for visual comparison against the original to ensure accuracy. Mean species shapes were obtained by taking the species mean for each coefficient and reconstructing the outline. Because eigenshape analysis requires equal spacing of points around the outline, a coordinate list of one hundred steps for each mean species shape was produced from all twenty EF coefficients. Principal components analysis was performed on the covariance matrix of the EF descriptors (EF-PCA) of mean species shape for both tissue types and axes scores were recorded until 95% of the total variance was captured. Eigenshape analysis (EGS) was performed on the standardized 100 step coordinate lists by using free software programs (MacLeod, 1999).

Four size measurements were taken for each specimen between the homologous landmarks (Fig. 1). Measurements between A–D and A–B were chosen for exocarp size and between B–E and B–C for receptacle size. These measurements not only capture outline size but also distance between the exocarp and receptacle margins. All individual measurements were standardized to one by the maximum value and species means were calculated.

Analysis of Morphometric Data

Datasets for further analysis then consisted of only the significant axes from the EF-PCA and EGS analyses, plus two size measurements for each tissue type and a mean angle of rotation for the exocarp. Initially, a cluster analysis, using a hierarchical model based on between-group linkage and squared Euclidean distance, was performed in SPSS for Windows 9.0 (SPSS Inc., 2000). The resulting dendrograms were then rearranged for easy visual comparison with likelihood phenograms rooted with *Q. alba*, maintaining distances between nodes.

The datasets were also analyzed with the PHYLIP v. 3.6 program, ContML Felsenstein, 1973, 1981, 2000), under the conditions of continuous data, global rearrangements, and ten random addition sequences. The resulting maximum likelihood tree was then taken as the most likely transformation series of shape change, with branches leading to particular clades explaining a common degree of change. Node support was analyzed by conventional bootstrapping methods (Felsenstein, 1985).

Molecular Data

Total DNA was extracted from fresh leaf samples in the field using Qiagen DNEasy preps (Qiagen Inc.; Santa Clarita, CA), precipitated, dried and shipped back to the laboratory. Product for both ITS1 & 2 and the 5.8S regions of the rDNA were obtained using direct PCR and universal primers (Baldwin, 1992). Sequence reactions were prepared using the ABI Prism Dye Terminator Cycle

Sequencing Reaction Kit (The Perkin-Elmer Corporation, 1999). Occasionally, the presence of sequence heterogeneity would require subsequent cloning of PCR product (TA Cloning Kit, Invitrogen; Carlsbad, CA). Clones were chosen by their length and sequence similarity within the context of this study and previous studies of the Fagaceae (Manos et al., 1999; in press). Sequences were verified from both directions and all questionable and informative calls in Sequencher (GeneCodes; Ann Arbor, MI) were compared directly against the chromatograms.

Sequences were aligned by eye and total length was 645 bases. Numerous indels were present. Fourteen were coded absent or present, nine of which were parsimony-informative. Single base pair extensions were removed from the analysis. Both parsimony and maximum likelihood reconstructions of phylogenetic structure were performed using PAUP* 4.0b8 (Swofford, 2001). Twenty-five random addition sequences were performed and heuristic searches were allowed to swap to completion. Characters were weighted equally. Branch lengths not significantly different from zero were collapsed.

Combined Analysis

Combined parsimony analyses were performed using the raw molecular sequence data and matrix representations (Brooks, 1990; Baum, 1992; Doyle, 1992; Ragan, 1992) for each of the four separate morphometric analyses: 1) EF-PCA cluster; 2) EF-PCA ContML; 3) eigenshape (EGS) cluster; and 4) EGS ContML. In modification of standard matrix representation parsimony, "MRP" (Bininda-Emonds and Bryant, 1998), inferred morphological difference between nodes from the maximum likelihood phenogram was applied as a weighting scheme. These weights were divided by the maximum inferred morphological difference on an internal branch of each phenogram to standardize the weighting scheme between datasets. Because no a priori argument exists for weighting matrix elements, relative weighting by inferred morphological difference and standardization was deemed appropriate. Under this method, nodes with little inferred morphological difference have a weight near zero and thus contribute little to the analysis.

All nodes in the four unrooted morphometric transformation series were included in the MRP datasets, thus 45 characters (2n-3) were contributed by each dataset and incorporated directly with the ITS molecular sequence data. Further exploration of this method for incorporating continuous data into a combined analysis and attempts at simultaneous maximum likelihood analyses are currently being pursued. Standard congruency tests, such as the ILD (Farris et al., 1995), are inappropriate because of the different types of characters or elements in each dataset. Until an adequate test can be developed, we present both separate and combined analyses.

Bootstrapping was performed in two ways: 1) treating the elements of the MRP datasets like conventional characters and 2) bootstrapping the molecular and morphometric datasets separately, producing phenograms for each morphological bootstrap replicate, converting it into a MRP dataset and then subsequently performing a combined analysis with a randomly chosen molecular bootstrap replicate. One hundred bootstrap replicates were used in both cases. The process of separate bootstrapping was necessary because using MRP data sets as independent characters imposes an inherent nesting of taxa (Purvis, 1995), therefore violating the assumption of character independence. Bootstrapping such a dataset would determine the influence of exclusion of random nodes on the analysis and not explore the original variance in the morphometric data, as the bootstrap was originally intended (Felsenstein, 1985).

Congruence between the datasets is difficult to assess for two reasons. Firstly, given our current understanding of morphological evolution as it relates to morphometric change (Felsenstein, 1988), we must accept the ContML reconstructions of fruit shape variance as phenograms and not phylogenetic hypotheses. Therefore, combining the MRP datasets with the molecular data has more in common with adding two complex ordered characters to the molecular dataset than to combining two separate and complete sources of phylogenetic information. Exploring the impact of accepting a few such characters from a second independent source, even with mixed phylogenetic signal, seems necessary. These morphometric characters should also be incorporated into a complete cladistic analysis of morphology. Only then do questions

of congruence between datasets seem appropriate.

Secondly, MRP elements cannot be considered independent characters as discussed previously. The bootstrap or partition homogeneity tests require sets of independent characters. Using MRP datasets for both molecular and morphometric partitions does not overcome the lack of independence among matrix elements. Despite these limitations, the ILD test on the combined dataset, assuming the same method and weighting scheme as described above, was performed. An additional ILD test on a combined dataset comprised of MRP datasets for both molecular and morphometric topologies was also performed. Matrix elements were weighted by branch length and standardized by the longest internal branch, following methods used for the morphometric data. Given the violations discussed above, alternative strategies for testing the congruency between such datasets should be explored.

Comparative Analysis

To identify significant differences in evolutionary pace between the two datasets, we compared the inferred amount of change at critical nodes for each dataset. Each of the separately bootstrapped datasets from the previous test was mapped onto the best phylogenetic reconstructions obtained from both the molecular and combined analyses. Branch lengths at well-supported nodes (>50% bootstrap value) from each replicate and each dataset were estimated using the parsimony accelerated and delayed transformation and minimum F character optimizations (Farris, 1972; Swofford and Maddison, 1987) and the default maximum likelihood HKY model (Hasegawa et al., 1985). They were standardized by the total tree length from each replicate for direct comparison among replicates and between data sets. Only variable sites were included in these estimates. The mean relative branch length for each dataset was calculated and frequency distributions were compared. Because many of the distributions were not normal, Mann-Whitney U pair-wise tests of significance were performed for corresponding nodes between datasets. Branch length estimates using the bootstrap technique have been shown to be reliable, even when the distributions are not normal (Sitnikova, 1996).

RESULTS

Morphometric Data

Exocarp.—More than 95% of shape variance was captured by EGS analysis on the first two axes while EF-PCA required an additional two axes to capture equal amounts of variance (Fig. 2). Even with orientation removed, ER and acorn fruit types were generally separated by both techniques, suggesting distinctive shape changes that occur with the reduction of the exocarp in the ER fruit type. Within each of these fruit types, exocarps forming simple curves were distinguished from ones with more sinusoidal shapes.

In cluster analyses of shape, including size and orientation (Figs. 3A,C), only the large and thickened exocarp of *L. revolutus* (#14) was distinguished in both analyses from other acorn fruits (Fig. 3C), while EF-PCA additionally separated the sharply curved *L. havilandii* (#6, Fig. 3A). *Lithocarpus keningauensis* (#19), with an almost inverted and sinusoidal exocarp, was placed halfway between the two fruit types. The EF-PCA groupings of ER fruited taxa more closely followed traditional taxonomic classifications than the EGS groupings. Sections *Lithocarpus* (black squares, Fig. 3) and *Synaedrys* (black circles, Fig. 3) formed groups, although two previously unclassified taxa, *L. ruminatus* (#21) and *L. rotundatus* (#20), were placed in the "wrong" group, based upon current sectional limits {Camus, 1952–1954 #2196}. The EGS grouping mixed the two sections along with the previously unclassified taxa.

The restricted maximum likelihood phenograms (ContML) of morphometric variance, including size and orientation, were nearly identical in topology (Figs. 3B,D). The two descriptors (EF-PCA and EGS) differed mainly in branch length and little in topology. The grouping of *L. revolutus* (#14) and *L. lampadarius* (#12) was a significant improvement over the cluster analysis, since many other aspects of morphology support this close relationship {Soepadmo, 1970 #2188}. The ER-fruited taxa were strongly separated from the acorn-fruited ones, with the exocarp morphologies of *L. sericobalanus* (#17) and *L. echinifer* (#18) suggested as intermediate between the two types. *Lithocarpus keningauensis* (#19), instead of being separated from the other ER fruit types as an idiosyncratic morphology, was nested in the
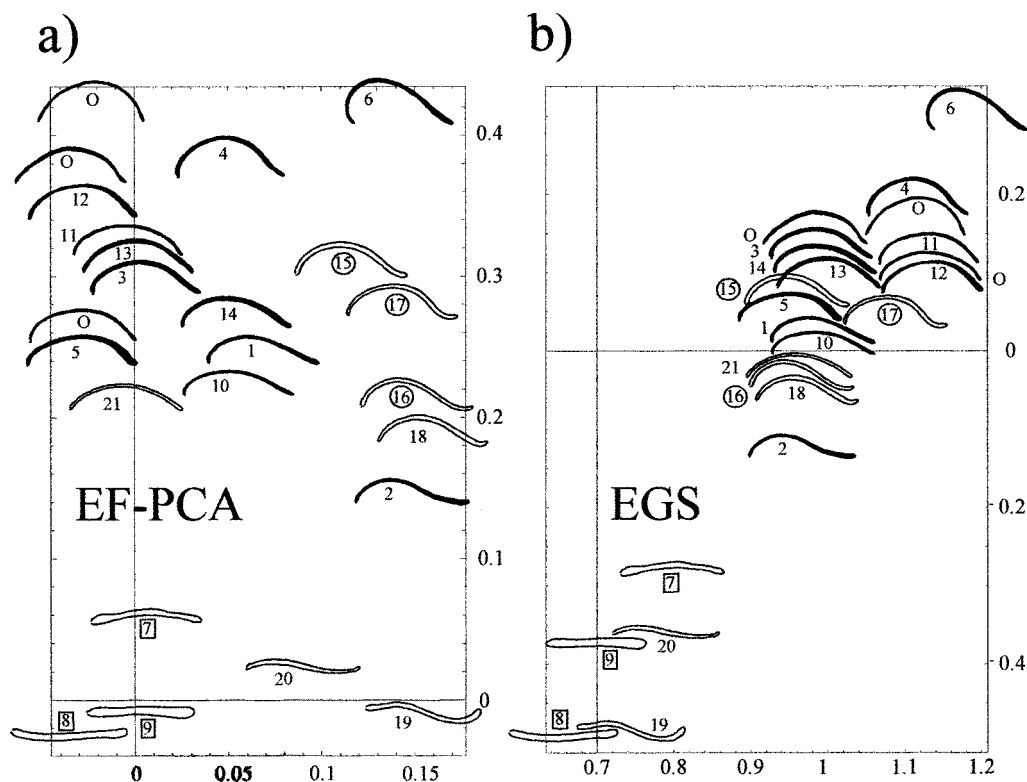
FIGURE 2.   Position of mean exocarp shape on the first two axes of a) principal components analysis of the first twenty harmonics of an elliptic Fourier transformation (EF-PCA) and b) an eigenshape (EGS) analysis. All outlines were standardized for size, starting and relative position, and orientation. 85% and 98% of total variance was described, respectively. ER-fruited taxa are clear and acorn-fruited taxa are black. Shapes are numbered according to Appendix A. Labels for section *Lithocarpus* are enclosed within squares, while section *Synaedrys* are enclosed within circles.

ER group and section *Lithocarpus*. Both ContML groupings disagreed with current sectional limits. Bootstrap values for the two descriptors were not highly correlated with branch length (Figs. 3B,D). Both descriptors appeared to possess significant structure, as likelihood values for the best topology were much greater than 100 random topologies.

Receptacle.—The EF-PCA and EGS analyses distinguished the two fruit types on the first two axes (Figs. 4A,B). The latter analysis required more axes (6 vs. 5) to capture 95% of total variance. The deeply invaginated and thick walled ER fruits of section *Lithocarpus* plus *L. keningauensis* (#19) form a tight cluster in both analyses and were more clearly distinct from section *Synaedrys* in the EF-PCA analysis. *Lithocarpus ruminatus* (#21), with its thickened base and slender enclosing upper extensions, was obviously unique in the genus, although it lies close to *L. revolutus* (#14) in the EGS analysis. The acorn fruit

types with thin and flattened receptacles, are tightly grouped in both analyses, with small variations in curvature and thickness.

Cluster analysis of receptacle shape descriptors provided abundant structure within acorn fruits, clear separation between the two fruit types, and largely congruent divisions between ER sections (Figs. 5A,C). In the EF-PCA cluster analysis, *L. clementianus* (#3), *L. luteus* (#13), *L. lucidus* (#5), and *L. lampadarius* (#12), were placed approximately equidistant between the acorn and ER fruit types (Fig. 5A), while EGS descriptors of *L. sericobalanus* (#17) and *L. revolutus* (#14) also fell into this group (Fig. 5C). The highly divergent morphologies of *L. revolutus* (#14) and *L. ruminatus* (#21) were grouped together by the EF-PCA descriptors but widely separated by the EGS descriptors. *Lithocarpus keningauensis* (#19), highly divergent in exocarp shape, clustered within section *Lithocarpus*.
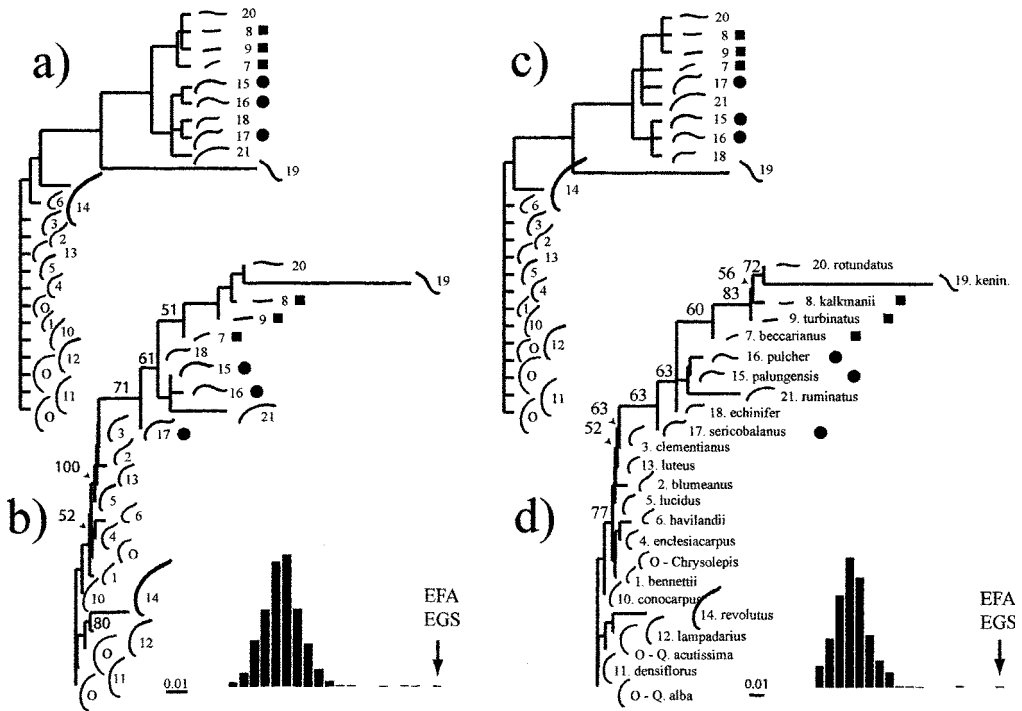
FIGURE 3. Phenograms of morphometric descriptors for mean exocarp shape. (a) Cluster analysis and (b) restricted maximum likelihood analysis (ContML) of four axes from EF-PCA; (c) Cluster analysis and (d) ContML analysis of two axes from EGS. Both analyses also included two size measurements and one measure of orientation. Histograms represent ContML scores of one thousand random trees and arrows point to scores of observed ContML phenograms. Mean outline shape for each species is shown in the position of each OTU and numbers correspond to those in Appendix A. Members of section *Lithocarpus* are marked with black squares while members of section *Synaedrys* are marked with black circles. Bootstrap values (>50%) are shown on the ContML phenograms.

The ContML phenograms were similar to the cluster analyses but with several interesting differences (Figs. 5B,D). The intermediate types did not form a distinct group but rather a stepwise transition between acorn and ER-fruited taxa. In the EF-PCA, *L. revolutus* (#14) with *L. lampadarius* (#12) were grouped together, which is appropriate as discussed for the exocarp. In the EGS results however, *L. ruminatus* (#21) was placed between the two taxa (Fig. 5D). The two main sections with ER-fruited taxa were separated on both ContML phenograms but only section *Lithocarpus* for the EF-PCA data formed a unified clade. Section *Synaedrys* formed a grade in both analyses but was interspersed with *L. rotundatus* (#20) and *L. ruminatus* (#21) for the EF-PCA data and with *L. rotundatus* (#20) and *L. echinifer* (#18) for the EGS data. Nodes among ER-fruited taxa were well supported by bootstrap values while little support existed among acorn-fruited taxa. A

large amount of hierarchical structure is also apparent in the data.

Molecular Data

The monophyly of individuals representing several taxa was tested by sampling multiple accessions across their geographic range whenever possible and performing preliminary reconstructions. No polyphyletic taxa were present in this analysis and the dataset was reduced to single exemplar sequences to facilitate direct comparison with the morphometric data, which only included mean shapes for each taxa.

A total of 79 parsimony-informative characters (50 with the outgroup excluded) were found in the pruned dataset. Two equally-parsimonious trees (264 steps, CI = 0.72, RCI = 0.49) were found, differing only in the relationship among three acorn-fruited taxa (*L. blumeanus*, *L. enclesiacarpus*, and *L.*
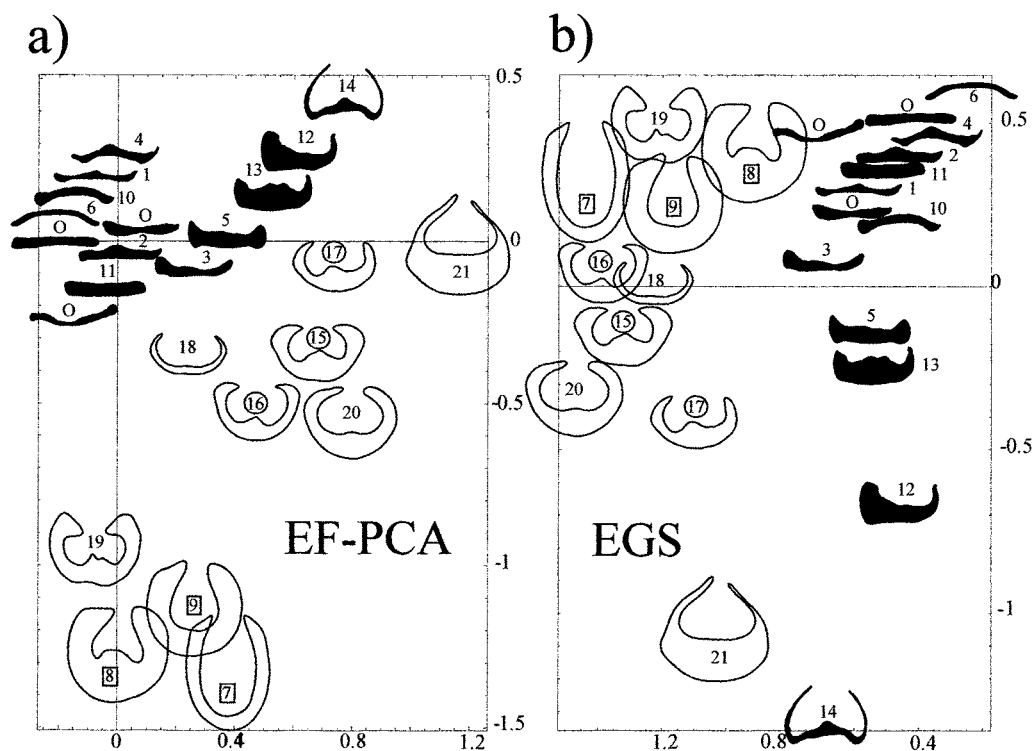
FIGURE 4.   Position of mean receptacle shape on the first two axes of (a) principal components analysis of an elliptic Fourier transformation (EF-PCA) and (b) an eigenshape (EGS) analysis. All outlines were standardized for size, starting point, relative position, and orientation. 86% and 76% of total variance was described, respectively. ER-fruited taxa are clear and acorn fruited taxa are black. Shapes are numbered according to Appendix A. Labels for section *Lithocarpus* are enclosed within squares, while section *Synaedrys* s.s. are enclosed within circles.

havilandii). Numerous transitions from acorn fruit morphology to ER fruit morphology can be inferred from this reconstruction, although only two are well supported (Fig. 6). Section *Lithocarpus* was monophyletic while the clade formed by section *Synaedrys* also included *L. keningauensis*.

Within the context of this study, the genus *Lithocarpus* was not monophyletic, as *Chrysolepis chrysophylla* was well-supported (76% bootstrap value) between the Bornean taxa and the North American disjunct, *L. densiflorus* (Fig. 6). Given these results and those from a comprehensive family level study (Manos et al., in press), *L. densiflorus* appears to be distinct from the Asian taxa within the genus. The taxonomic status of this relictual species requires further study.

Combined Analysis

No current statistical test of dataset congruence exists for testing a standard molecular dataset and a MRP dataset because of their different statistical properties, as discussed in the methods. A standard ILD test suggests that the two datasets should not be combined but the significance level is marginal ($p = 0.05$). Performing an ILD test on combined MRP datasets also indicated significant incongruence ($p < 0.01$). As discussed in the methods, "incongruence" between the molecular and morphometric data is also difficult to interpret because of the phenetic nature of the ContML topologies. The most obvious difference between the topologies obtained from the separate analyses is the placement of *L. keningauensis* (Figs. 3, 5, and 6). The fruit morphology in this extremely rare taxon is very unusual and the incongruity between these datasets may suggest a hybrid origin. Overall, in the exploratory spirit of this study, incorporating the morphometric data into a combined analysis seemed worthwhile.

The combined analyses using MRP datasets from the cluster phenograms (Figs. 3A,C and 5A,C) both produced a
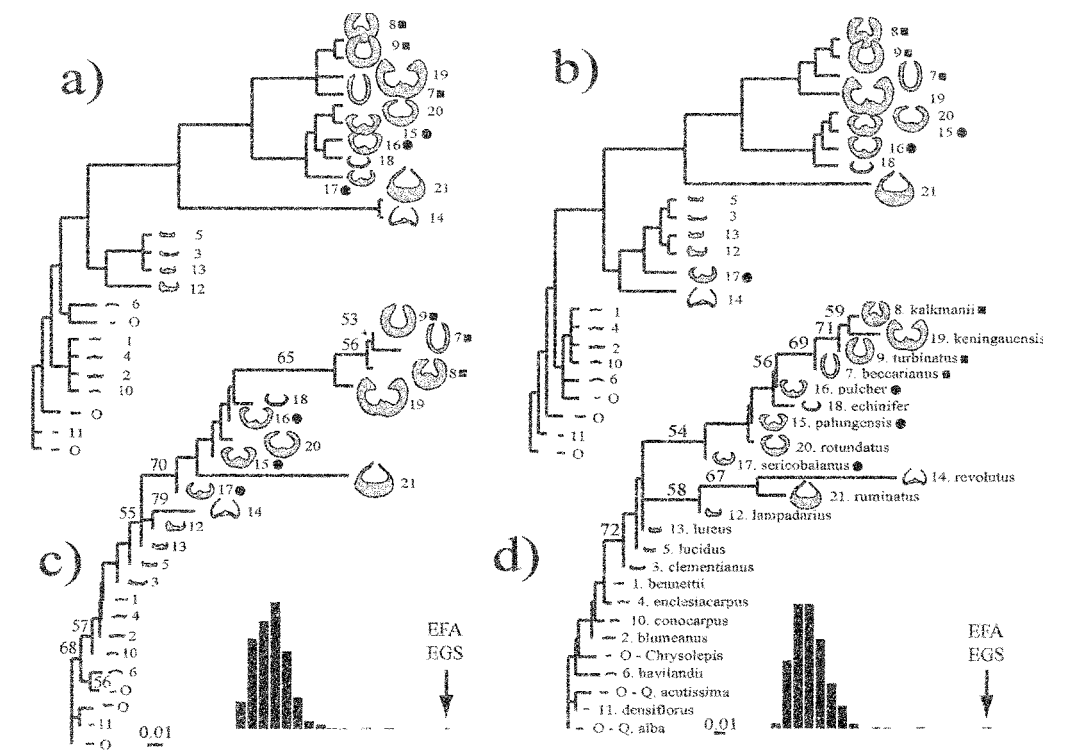
FIGURE 5. Phenograms of morphometric descriptors for mean receptacle shape. (a) Cluster analysis and (b) restricted maximum likelihood analysis (ContML) of five axes from EF-PCA plus two size measurements; (c) Cluster analysis and (d) ContML of six axes from EGS plus two size measurements. Histograms represent ContML scores of one thousand random trees and arrows point to score of each ContML phenograms. Mean outline shape for each species is shown in the position of each OUT and numbers correspond to Appendix A. Members of section *Lithocarpus* are marked with black squares while members of section *Synaedrys* are marked with black circles. Bootstrap values (>50%) are shown on the ContML phenograms.

single most parsimonious tree while combined analyses using the ContML phenograms (Figs. 3B,D and 5B,D) for EF-PCA and EGS data produced three and six equally-parsimonious trees, respectively. When each of the separate and combined datasets was mapped onto the different topologies, little difference in scores were apparent, although each dataset did score best on its own topology (Table 1). Since choosing a "best" method for combining the datasets cannot be done objectively, the EF-PCA phenograms produced by the ContML method were chosen because of

TABLE 1. Tree scores for all data sets, separate and combined, when mapped onto the best topology generated from each analysis. Consistency indices are shown in parentheses. Rows 2 and 3 are positive likelihood scores from ContML (Felsenstein, 2000).

|	Topology				
Data	ITS alone (2 trees)	ITS + EF-PCA cluster (1 tree)	ITS + EF-PCA CML (3 trees)	ITS + EGS cluster (1 tree)	ITS +EGS CML (6 trees)
ITS	264 (0.72)	265 (0.72)	265 (0.70)	272 (0.70)	267 (0.72)
EF-PCA	463	492.8	486.6	509.6	496.4
EGS	356	378.4	379.1	391.8	382.8
ITS + EFPCA cluster	302 (0.70)	297 (0.71)	297 (0.71)	298 (0.71)	298 (0.71)
ITS + EFPCA CML	302 (0.70)	298 (0.70)	298 (0.70)	301 (0.70)	299 (0.70)
ITS + EGS cluster	317 (0.69)	308 (0.71)	309 (0.71)	306 (0.71)	310 (0.70)
ITS + EGS CML	316 (0.68)	311 (0.69)	311 (0.69)	314 (0.69)	309 (0.70)
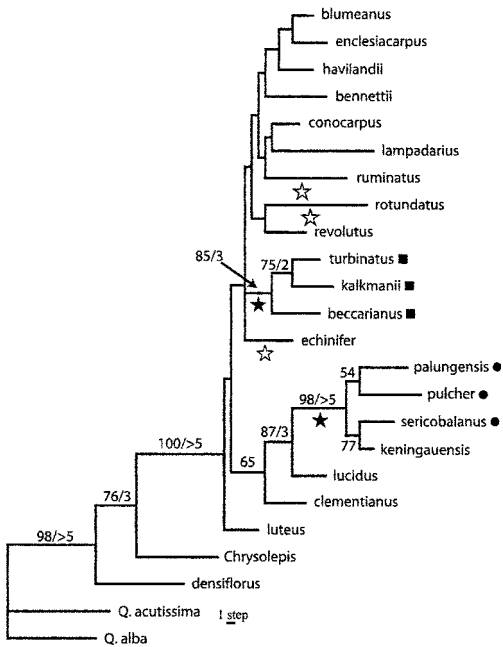
FIGURE 6. One of two equally-parsimonious trees for ITS sequence data (264 steps, CI = 0.72, RCI = 0.49) with ≥50% bootstrap value/>1 decay index. 636 characters were used, of which 79 were parsimony-informative, 50 excluding outgroup. Black stars indicate well-supported transitions from acorn to ER-fruited taxa; grey stars, poorly-resolved transitions. Black squares indicate members of section *Lithocarpus*; black circles, members of section *Synaedrys*.

FIGURE 7. Combined analysis of ITS and EF-PCA ContML MRP characters. Single most parsiminous tree (score = 298, CI = 0.70, RCI = 0.47) is shown. A total of 732 characters (121 informative; 89 without outgroup) were used. Bootstrap support was estimated in two ways: conventional bootstrapping of the combined dataset (shown after slash) and separate bootstrapping with subsequent combination (shown before slash). The black stars indicate inferred transitions to ER fruit type from acorn fruit type, while the white star indicates a reversion to the acorn fruit type. Black squares indicate members of section *Lithocarpus*; black circles, members of section *Synaedrys*.

their general agreement with current taxonomic limitations and appropriate placement of several key taxa. Between the three equally-parsimonious trees (score = 298.03, CI = 0.70, RC = 0.47) produced by the combined analysis, the only difference among them is the placement of *L. luteus* (Fig. 7), being 1) sister to all Bornean taxa, 2) unresolved among all Bornean taxa, and 3) sister to the clade containing section *Synaedrys*. To simplify matters, the unresolved position for this taxon was used for further analysis and discussion.

Estimates of bootstrap support, using either the conventional or the method described above, were similar, although the latter method supported two additional nodes (Fig. 7). Like the molecular analysis, two acorn-fruited taxa (*L. clementianus* and *L. lucidus*) were well-supported basally to the members of section *Synaedrys* + *L. keningauensis*. In contrast to the molecular tree, all remaining ER-fruited taxa formed a clade, with *L. ruminatus* as sister to (section
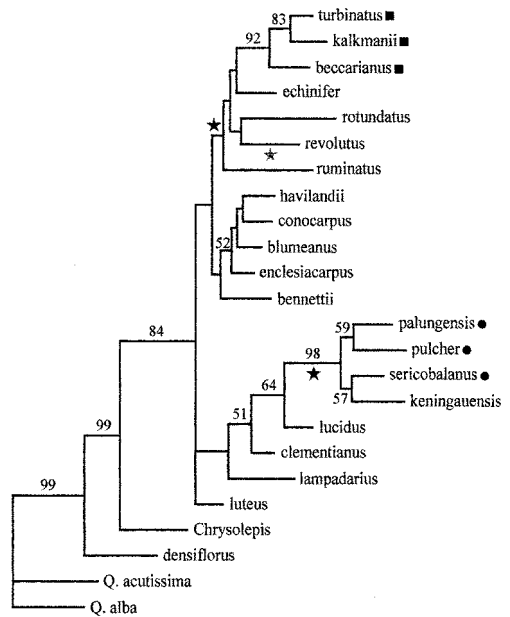
Lithocarpus + *L. echinifer* and *L. rotundatus*). The monophyly of several acorn-fruited taxa was an additional well-supported node not found in the separate molecular analysis.

Comparison of Inferred Molecular and Morphometric Change

Given our current inability to objectively accept or reject the combined analysis, the comparative analysis was performed on both the separate molecular topology and the combined molecular/EF-PCA ContML topology. Only well-supported nodes were examined. Generally, the method of character state optimization or morphometric description did not influence the relative patterns between data sets (Figs. 8–9). The difference in topology between the two analyses only influenced inferences concerning the ingroup, as would be expected, as
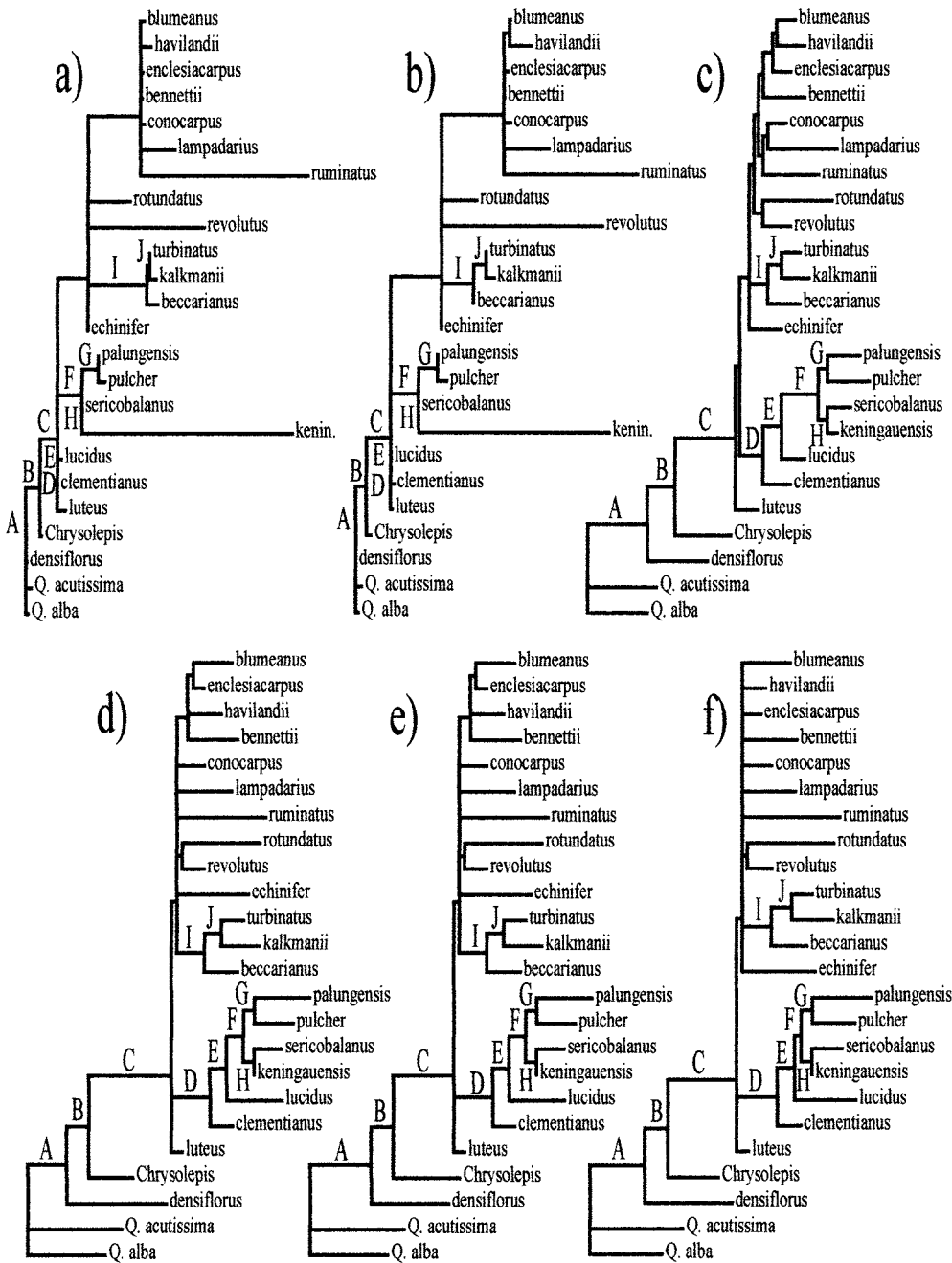
FIGURE 8.   Inferred phylogram for each dataset on best reconstruction of molecular data. (a) EF-PCA, (b) EGS, (c) ITS using ACCTRAN character optimization, (d) ITS using DELTRAN, (e) ITS using MinF, and (f) ITS using HYK model for maximum likelihood. Well-supported nodes are labeled A–J.

outgroup/ingroup relationships are identical.

The inferred amount of change between ITS sequence and morphometric descriptors was significantly different at most well supported nodes (Figs. 10–11). The large amount of molecular divergence between the *Quercus* taxa and the taxa of subfamily Castaneoideae has occurred without detectable change in fruit shape (Figs. 8–11, node a). As would be expected, the inferred amount of change was greater with
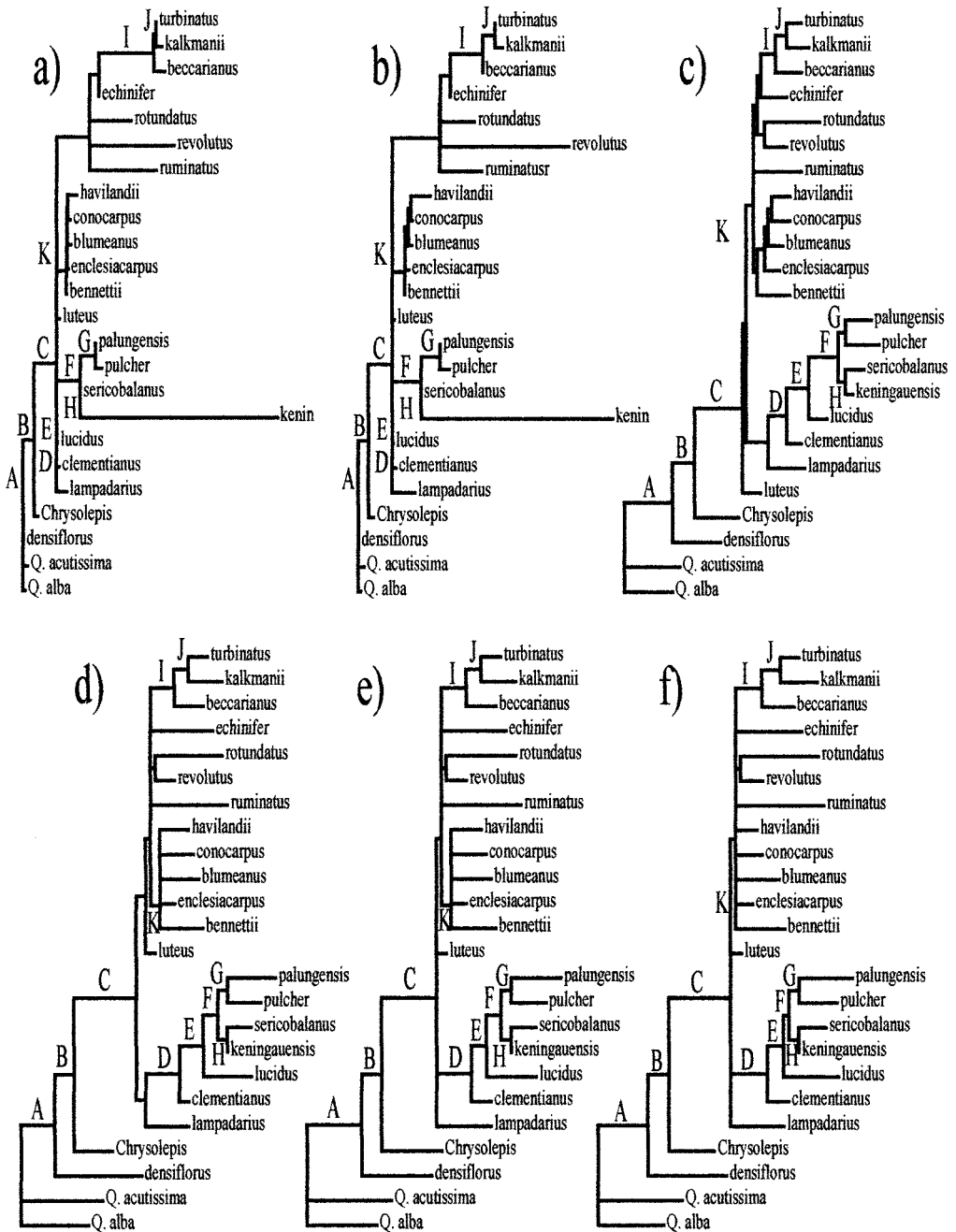
FIGURE 9. Inferred phylogram for each dataset on best combined reconstruction of molecular and morphometric data. (a) EF-PCA, (b) EGS, (c) ITS using ACCTRAN character optimization, (d) ITS using DELTRAN, (e) ITS using MinF, and (f) ITS using HYK model for maximum likelihood. Well-supported nodes are labeled A–K.

accelerated transformation (ACC) rather than delayed transformation (DEL) character optimization. Similarly, the inferred change at the node separating the Bornean species from the outgroups + *L. densiflorus* was greater for the molecular data,

although in this case, the amount of morphometric change was also appreciable (Figs. 10–11, node c). At node b, separating *Quercus* + *L. densiflorus* and the Bornean taxa + *Chrysolepis*, molecular and morphological change were relatively similar (Figs. 10–11,
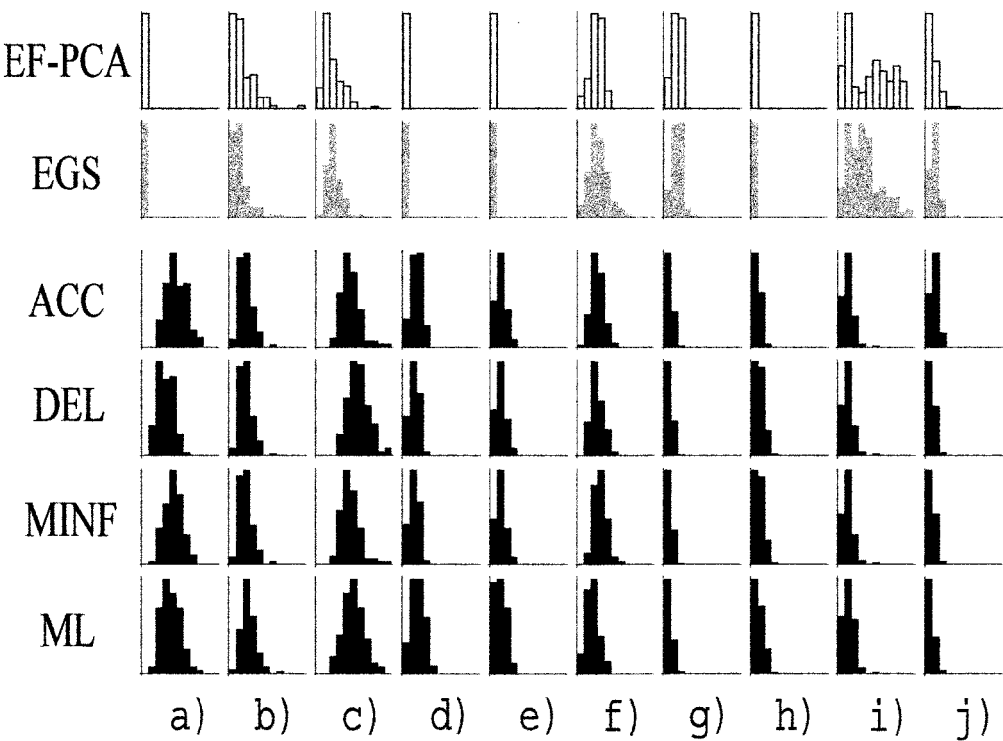
FIGURE 10. Comparison of inferred branch lengths on best molecular reconstruction. Each dataset was boot-strapped separately and mapped on the molecular tree. Distributions indicate range of inferred change for each well-supported node from 0–10% total variance, relative to tree length. Labels correspond to the nodes in Figure 8. The EF-PCA data is shown in white bars, the EGS in grey bars, and the ITS data, under four different assumptions of character optimization, in black bars.

node b). The range of variance in the EF-PCA dataset revealed by the bootstrap analysis for this node was quite large.

The two nodes supporting *L. clementianus* and *L. lucidus* sister to section *Synaedrys* (d and e) suggested morphological stasis while a moderate amount of molecular change has occurred (Figs. 10–11, nodes d and e). At the node separating acorn and ER-fruited taxa in this clade (Figs. 8–9, node f), the relative amount of inferred change depended on the assessed topology and type of character optimization used. The combined analysis suggested greater morphological under all models, particularly for the EGS dataset (Figs. 10–11, node f). Using the ITS tree, maximum likelihood inferred the least and MinF the most molecular change at this node, while inferences from ACCTRAN and DELTRAN optimization were indistinguishable from either morphometric descriptor. Within section *Synaedrys*, the node grouping *L. pulcher* and *L. palungensis* (Figs. 8–11, node g) suggested greater morphological change while the node grouping *L.*

sericobalanus and *L. keningauensis* (Figs. 8–11, node h) suggested greater molecular change.

Morphological change inferred at the node supporting the members of section *Lithocarpus* (Figs. 8–11, node i) was much greater than molecular change for all models and topologies. Within the clade (Figs. 8–11, node j), small amounts of change were apparent in both datasets. The bimodal distribution of branch lengths inferred for the EF-PCA dataset at node i suggested an unequal distribution of variance among the morphometric characters.

DISCUSSION

Morphometric Descriptors

The shape descriptors chosen for this study capture relevant phenotypic variation. The two main fruit types, acorn and ER, are clearly distinguished and form taxonomically reasonable groups, largely in agreement with current definitions. Both morphometric
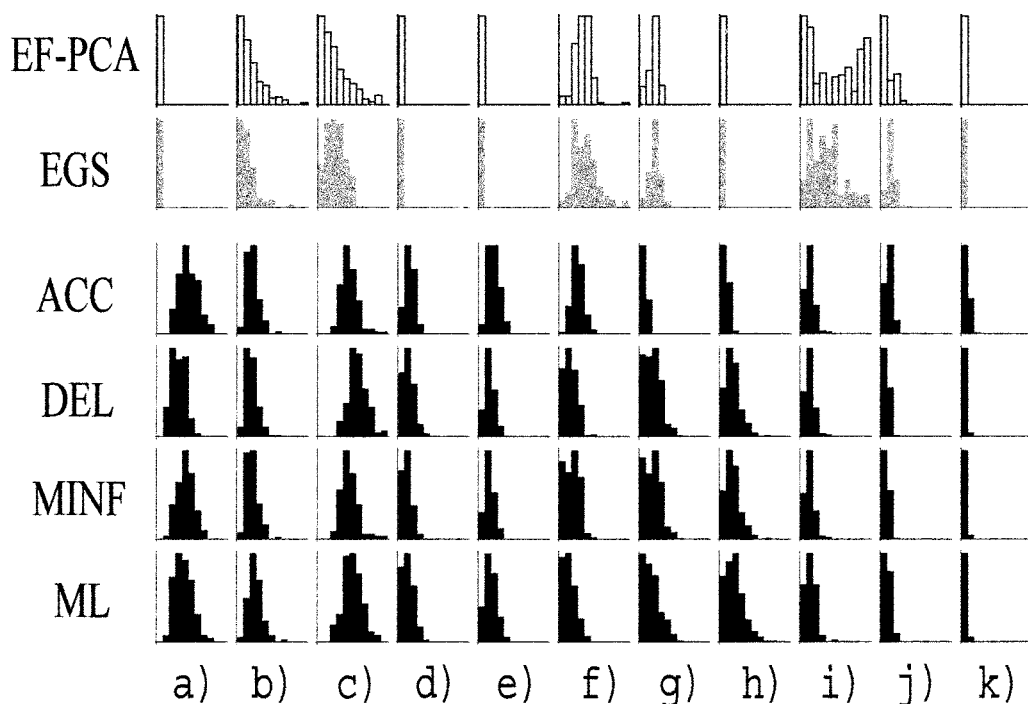
FIGURE 11. Comparison of inferred branch lengths on best combined reconstruction. Each dataset was boot-strapped separately and mapped on the combined tree. Distributions indicate range of inferred change for each well-supported node from 0–10% total variance, relative to tree length. Labels correspond to the nodes in Figure 9. The EF-PCA data is shown in white bars, the EGS in grey bars, and the ITS data, under four different assumptions of character optimization, in black bars.

methods, EF-PCA and EGS, are effective in describing important shape variation and produce similar results. The difference in the relative efficiency of the two methods—four vs. two major axes for the exocarp, and five vs. six for the receptacle, respectively—probably lies in the relative complexity of the two shapes. The EF-PCA analysis transforms the change in x and y coordinate lists separately while EGS transforms them simultaneously. The exocarp outline, which consists of simple curves, contains less variation, which is probably more highly correlated between the two coordinate systems, thus generally requiring fewer axes in the EGS analysis.

The relative success of any morphometric analysis will depend greatly on the relevance of the shape variation being described to the questions being addressed. Choosing a morphological feature appropriate to the level of the study is an essential first step. This feature must meet all traditional homology criteria (Roth, 1984; Roth, 1991) plus geometric aspects of rotation, size, and starting point (Crampton, 1995; Ferson et al., 1985). The feature should include both taxonomically

and phylogenetically important shape variation. The two methods used in this study will not be useful for all purposes, therefore we would encourage initial exploration of several morphometric techniques (Rohlf and Bookstein, 1990; Ray, 1992; Rohlf, 1998a; Borkowski, 1999).

The restricted maximum likelihood estimations of morphometric transformation, using ContML (Felsenstein, 2000), provided less traditional grouping structure than the cluster analyses but contained several advantages: 1) placement of *L. revolutus* with *L. lampadarius* for both exocarp and receptacle shape; 2) the placement of *L. keningauensis* within the ER-fruited taxa for exocarp, instead of being transitional between the two types; 3) phenetic distances among acorn-fruited taxa seem to be exaggerated in the cluster analyses, relative to differences between fruit types and among ER-fruited taxa; and 4) ContML phenograms are not ultrametric and uncertainty is expressed by near-zero branch lengths along a grade of taxa. The results from the combined analysis with the molecular data did not demonstrate

any significant differences for the different morphometric phenograms. The ContML phenogram of the EF-PCA data was chosen merely to simplify further analysis and discussion.

The use of a Brownian motion model of neutral evolutionary change is fairly robust in estimating independent contrasts of continuous characters under models that violate assumptions of neutrality (Diaz-Uriarte and Garland, 1996). Results from this model are comparable or better than other models at estimating independent contrasts under various simulated conditions (Diaz-Uriarte and Garland, 1998; Martins, 1996) and in testing patterns of morphometric variation against different macroevolutionary models (Mooers et al., 1999). Although neutral evolutionary change of fruit type in *Lithocarpus* should not be assumed, this model appears to be sufficiently robust in the absence of more appropriate models.

Overall, the use of continuous quantitative shape descriptors appears to be powerful in distinguishing phenetic differences among groups. Cluster analyses of shape variation could provide objective criteria for traditional taxonomic groupings but may provide unrealistic information about the morphometric relationships among groups. The use of multidimensional axes as independent characters in a restricted maximum likelihood analysis also provides groupings based upon morphometric similarity but more accurately captures subtle relationships among taxa and relative distances among groups. Although these phenograms should not be accepted as a phylogenetic hypothesis, they can be used as a morphometric transformation series (sensu Mickevich, 1982). The incorporation of these transformation series would then be analogous to a suite of correlated and ordered characters representing the morphometric similarity among the study taxa.

Molecular Phylogeny

Parsimony analysis of ITS sequences strongly supports two clades containing ER-fruited taxa. One consists entirely of ER fruited taxa and can be defined taxonomically as section *Lithocarpus* (*L. turbinatus*, *L. beccarianus*, and *L. kalkmanii*), while the other consists of both acorn and ER fruited taxa (*L. lucidus*—acorn, sister to section *Synaedrys*

sensu lato). These relationships suggest that the ER fruit type has been derived at least two times in the evolutionary history of the genus. The unresolved positions of three other ER-fruited taxa, *L. echinifer*, *L. rotundatus*, and *L. ruminatus*, weakly suggest multiple separate derivations.

Combined Analysis

The use of MRP coding to combine the morphometric transformation series with the molecular data appears to be informative. The most parsimonious trees support two separate derivations of the ER fruit type, placing the three ER-fruited taxa mentioned above in a single clade with section *Lithocarpus*. Although bootstrap support for this arrangement is not significant, the reduction of inferred derivations of the ER fruit type from five to two is more parsimonious. An additional node, grouping several acorn-fruited taxa together (*L. blumeanus*, *L. conocarpus*, *L. enclesiacarpus*, and *L. havilandii*), is also supported in the combined analysis. This grouping includes a wide variety of cupule types, from smooth and enclosed to bracteolate and reduced. Additionally, the ITS tree (Fig. 6) scores poorly when either the morphometric descriptors alone or the combined data are mapped onto it, while the scores for the ITS-EF-PCA combined trees are only one step longer when the ITS data is mapped onto them (Table 1).

The addition of 90 MRP elements from each set of two phenograms only increased the score of the resulting tree by only 40–50 "steps." Our conservative weighting scheme for these elements, which applies a maximum weight of one to the largest internal branch length and a relative weight to all other nodes, greatly minimizes the effect of nodes supported by little morphometric transformation. Different weighting schemes could be applied and should be explored when other information is available. An additional way to combine the datasets, instead of mixing raw molecular data with morphometric MRP datasets, is the conversion of the molecular data into a MRP dataset. The relative weight of each MRP dataset could be adjusted according to a priori assumptions or iterative approximation schemes, such as relative number of informative characters in each data set. We chose to use the raw molecular data to conserve the empirical weight

of the dataset, without having to impose a weighting scheme, but of course, this decision imposes a weighting scheme implicitly.

Testing congruence across the separate datasets for combined topology by ranking their scores on the resulting combined topologies provides an objective way of choosing the best morphometric descriptors in a particular situation. Although the suitability of congruence as the appropriate criterion for this purpose is questionable, it does generally satisfy the objectives of parsimony (Miyamoto and Fitch, 1995; Wiens, 1998). Because of the mathematical similarity of the two morphometric techniques used, the definitive selection of the best technique is difficult. The EGS descriptors appear to affect the combined analysis more strongly than the EF-PCA, particularly the EGS-cluster analysis (Table 1). The EF-PCA descriptor was chosen because of its greater relative agreement of the resulting combined analyses with each separate dataset. This technique cannot be expected to provide the best solution under all circumstances and examination of several different morphometric and analytical techniques should always be performed.

The use of conventional bootstrap methods on MRP datasets has been questioned on the grounds of lack of independence of matrix elements (Purvis, 1995; Bininda-Emonds et al., 1999). In our comparison of direct bootstrapping of MRP characters with separate bootstrapping and subsequent combining of datasets, we found that the direct bootstrapping technique supports two more nodes than separate bootstrapping, with generally higher values at all nodes. Because conventional bootstrapping of the MRP dataset does not assess the original variance, but merely the robustness of the hypothesis against loss of supporting nodes, we feel that separate bootstrapping and subsequent combination is necessary to avoid over-estimation of support.

Rates of Evolution

Given the best phylogenetic reconstruction for the study group using either molecular data alone or a combined dataset, inferred morphological and molecular change was seldom equal at most well-supported nodes. The difference in topology between the two phylogenetic analyses does not affect these differences, although it does affect the relative amount of change inferred within a single dataset, e.g. node g (Figs. 10–11). Although preliminary tests, where each bootstrap replicate is allowed to optimize the topology constrained of the well-supported nodes, suggest that the phylogenetic uncertainty in the reconstruction affects the amount of inferred change, the major patterns remain the same. This aspect of comparing datasets using this technique needs further examination.

The decoupling of morphological and molecular change between ingroup and outgroup reflects either convergent evolution or evolutionary stasis in fruit type between distantly related groups. Although the fossil record is limited for the Southeast Asian *Lithocarpus* and some difficulty exists in distinguishing between *Quercus* and *Lithocarpus* fruit fossils, the classic acorn fruit evolved 40 million years ago and remains present until modern times (Daghlian and Crepet, 1983; Manchester, 1994). This apparent stasis is not only apparent at the basal nodes but also among acorn-fruited taxa within the ingroup (nodes d and e, Figs. 8–11).

On the other hand, the derivation of the ER fruit type occurs rapidly with little correlated molecular change. This decoupling is most marked at the node subtending section *Lithocarpus* and involves a remarkable change in fruit wall shape and thickness. Despite the large amount of molecular change inferred at the node subtending section *Synaedrys*, the morphological change is relatively larger under most conditions of this analysis. Because of the large degree of molecular divergence between section *Synaedrys* and the remaining Bornean taxa, this split may suggest either great age of the group or an accelerated rate of molecular evolution. If morphological change does occur in a punctuated fashion, as suggested by most of the well-supported nodes of this study, then increasing age of a group may allow molecular change to slowly accumulate and eventually surpass the degree of morphological change.

Fruit Type Evolution

In the transition from acorn to ER-fruited taxa, the protective function of the fruit wall has shifted from the exocarp to the receptacle. The seed in the classic acorn fruit type is protected almost entirely by the exocarp, which forms a thin, brittle shell. In the extreme examples of the ER fruit type, the exocarp has

been reduced to a small, flattened disc and the thick, lignified receptacle encloses the seed. This morphological transition appears to have occurred in at least two separate lineages now present on Borneo and perhaps in other lineages currently found in Indochina (Manos et al., in press). This recurrent pattern suggests strong directional selection towards mechanical protection of the seed against predation. Further evidence for this selection can be found in the other tropical genus in the chestnut subfamily, *Castanopsis*, where parallel trends in fruit evolution exist (Camus, 1952–1954, Soepadmo, 1968a).

In the evergreen tree communities on the island of Borneo, synchronized and suprannual ("mast") fruiting often involves a wide range of woody taxa (Appanah, 1993). Numerous mechanisms causing this phenomenon have been suggested (Isagi et al., 1997; Kelly, 1994; Sork, 1993). Satiation of seed predators has been commonly proposed as the main mechanism (Janzen, 1974) and participation in large mast events has been shown to increase the percentage of seeds that successfully survive to germination (Curran and Webb, 2000). Little evidence suggests that the members of Fagaceae participate in this general masting event (Sakai, 1999). This lack of synchrony may be due to the inability of the family to rapidly mature fruit, which must occur to synchronize fruiting with masting members of the community.

The apparent morphological correlates with the ER fruit type are overall fruit size and seed volume, which may reflect greater investment by the parent tree in each seed because of the reduced risk of seed predation. The additional mechanical protection may also allow longer dormancy before germination (Ng, 1991) and reduce the effect of density dependent mortality (Givnish, 1999; Webb and Peart, 1999). Observations of *Lithocarpus* reproduction and regeneration remain vague (Kaul, 1989) but the evolution of the ER fruit type may coincide with an inability to participate in community-wide mast fruiting and high seed predation pressure.

REFERENCES

APPANAH, S. 1993. Mass flowering of dipterocarp forests in the aseasonal tropics. J. Biosci. 18:457–474.

BALDWIN, B. G. 1992. Phylogenetic utility of the internal transcribed spacers of nuclear ribosomal DNA in plants: an example from the Compositae. Mol. Phylogen. 1:3–16.

BARNETT, E. C. 1944. Keys to the species groups of *Quercus*, *Lithocarpus*, and *Castanopsis* of eastern Asia, with notes on their distributions. Tran. Bot. Soc. Edin. 34:159–204.

BAUM, B. 1992. Combining trees as a way of combining data sets for phylogenetic inference, and the desirability of combining gene trees. Taxon 41:3–10.

BININDA-EMONDS, O. R. P., AND H. N. BRYANT. 1998. Properties of matrix representation with parsimony analyses. Syst. Biol. 47:497–508.

BININDA-EMONDS, O. R. P., J. L. GITTLEMAN, AND A. PURVIS. 1999. Building large trees by combining phylogenetic information: a complete phylogeny of the extant Carnivora (Mammalia). Biol. Rev. Cambridge Philosophic. Soc. 74:143–175.

BORKOWSKI, W. 1999. Fractal dimension based features are useful descriptors of leaf complexity and shape. Can. J. For. Res 29:1301–1310.

BROOKS, D. R. 1990. Parsimony analysis in historical biogeography and coevolution-methodological and theoretical update. Syst. Zool. 39:14–30.

CAMUS, E. 1948. Les chenes. Monographie des genres *Quercus* et *Lithocarpus*, Atlas, vol. 3. 7:152–165.

CAMUS, E. 1952–1954. Les chenes. Encyl. Econom de Sylvic. 8:511–1196.

CANNON, C. H., AND P. S. MANOS. 2000. The Bornean *Lithocarpus* Bl. section *Synaedrys* (Lindl.) Barnett (Fagaceae): its circumscription and description of a new species. Bot. J. Linnean Soc. 133:343–357.

CRAMPTON, J. S. 1995. Elliptic Fourier shape-analysis of fossil bivalves-some practical considerations. Lethaia 28:179–186.

CRONIER, C., S. RENAUD, R. FEIST, AND J. C. AUFFRAY. 1998. Ontogeny of *Trimerocephalus lelievrei* (Trilobita, Phacopida), a representative of the Late Devonian phacopine paedomorphocline: a morphometric approach. Paleobiology 24:359–370.

CURRAN, L. M., AND C. O. WEBB. 2000. Experimental tests of the spatiotemporal scale of seed predation in mast-fruiting Dipterocarpaceae. Ecol. Monogr. 70:129–148.

DAGHLIAN, C. P., AND W. L. CREPET. 1983. Oak catkins, leaves and fruits from the Oligocene Catahoula

Formation and their evolutionary significance. Am. J. Bot. 70:639–649.

DIAZ-URIARTE, R., AND T. GARLAND. 1996. Testing hypotheses of correlated evolution using phylogenetically independent contrasts: Sensitivity to deviations from Brownian motion. Syst. Biol. 45:27–47.

DIAZ-URIARTE, R., AND T. GARLAND. 1998. Effects of branch length errors on the performance of phylogenetically independent contrasts. Syst. Biol. 47:654–672.

DOYLE, J. J. 1992. Gene trees and species trees-molecular systematics as one-character taxonomy. Syst. Bot. 17:144–163.

FARRIS, J. S. 1972. Estimating phylogenetic trees from distance matrices. Am. Nat. 106:645–668.

FARRIS, J. S., M. KALLERSJO, A. G. KLUGE, AND C. BULT. 1995. Constructing a significance test for incongruence. Syst. Biol. 44:570–572.

FELSENSTEIN, J. 1973. Maximum-likelihood estimation of evolutionary trees from continuous characters. Am. J. Human Gen. 25:471–492.

FELSENSTEIN, J. 1981. Evolutionary trees from gene frequencies and quantitative characters: finding maximum likelihood estimates. Evolution 35:1229–1242.

FELSENSTEIN, J. 1985. Confidence limits on phylogenies: an approach using the bootstrap. Evolution 39:783–791.

FELSENSTEIN, J. 1988. Phylogenies and quantitative characters. ARES 19:445–471.

FELSENSTEIN, J. 2000. PHYLIP (Phylogeny Inference Package) Version 3.6. University of Washington, Seattle.

FERRARIO, V. F., C. SFORZA, G. SERRAO, T. FRATTINI, AND C. DELFAVERO. 1996. Shape of the human corpus callosum in childhood-Elliptic fourier analysis on midsagittal magnetic resonance scans. Invest. Radiol. 31:1–5.

FERSON, S., F. J. ROHLF, AND R. K. KOEHN. 1985. Measuring shape variation of two-dimensional outlines. Syst. Zool. 34:59–68.

FORMAN, L. L. 1966a. Generic delimitation in the Castaneoideae. Kew Bull.:421–426.

FORMAN, L. L. 1966b. On the evolution of the cupules in the Fagaceae. Kew Bull. 18:385–419.

GIVNISH, T. J. 1999. On the causes of gradients in tropical tree diversity. J. Ecol. 87:193–210.

HASEGAWA, M., H. KISHINO, AND T. YANO. 1985. Dating the human-ape split by a molecular clock of mitochondrial DNA. J. Mol. Evol. 22:160–174.

ISAEV, M. A., AND L. N. DENISOVA. 1995. The computer programs for shape analysis of plant leaves in Mathematics, Computers, and Education, Pushchino.

ISAGI, Y., K. SUGIMURA, A. SUMIDA, AND H. ITO. 1997. How does masting happen and synchronize? J. Theor. Biol. 187(2):231–239.

JANZEN, D. H. 1974. Tropical blackwater rivers, animals, and mast fruiting by the Dipterocarpaceae. 4:69–103.

JENKINS, R. 1993. The origin of the Fagaceous cupule. Bot. Rev. 59:81–111.

JULIA, S., AND E. SOEPADMO. 1998. New species and new record of Lithocarpus Blume (Fagaceae) from Sabah and Sarawak, Malaysia. Gard. Bull. Sing. 50:125–150.

KAUL, R. B. 1987. Reproductive structure of Lithocarpus sensu lato (Fagaceae): cymules and fruits. J. Arn. Arb. 68:73–104.

KAUL, R. B. 1989. Fruit structure and ecology in paleotropical Lithocarpus (Fagaceae). Pages 67–86 in Evolution, Systematics, and Fossil History of the Hamamelida (P. R. Crane and S. Blackmore, eds.). Clarendon Press, Oxford.

KELLY, D. 1994. The evolutionary ecology of mast seeding. TREE 9(12):465–470.

KINCAID, D. T., P. J. ANDERSON, AND S. A. MORI. 1998. Leaf variation in a tree of Pourouma tomentosa (Cecropiaceae) in French Guiana. Brittonia 50:324–338.

KINCAID, D. T., AND R. B. SCHNEIDER. 1983. Quantification of leaf shape with a microcomputer and Fourier transform. Can. J. Bot. 61:2333–2342.

KUHL, F. P., AND C. R. GIARDINA. 1982. Elliptic Fourier features of a closed contour. Comp. Graph. Image Proc. 18:259–278.

LANGDON, D. M. 1939. Ontogenetic and anatomical studies of the Fagaceae and Juglandaceae. Bot. Gaz. 101:301.

LAURIE, C. C., J. R. TRUE, J. J. LIU, AND J. M. MERCER. 1997. An introgression analysis of quantitative trait loci that contribute to a morphological difference between Drosophila simulans and D. mauritana. Genetics 145:339–348.

LESTREL, P. E., A. BODT, AND D. R. SWINDLER. 1993. Longitudinal-study of cranial base shape changes in Macaca nemestrina. Am. J. Phys. Anthropol. 91:117–129.

LIAO, J.-C. 1969. Morphological studies on the flowers and fruits of the genus Lithocarpus in Taiwan. Nat. Taiwan Univ. Mem. Agri. 10:1–113.

LOHMANN, G. P., AND P. N. SCHWEITZER. 1990. On eigenshape analysis in Proceedings of the Michigan morphometrics workshop (F. J. Rohlf, and F. L. Bookstein, eds.). University of Michigan Museum of Zoology, Ann Arbor.

MACLEOD, N. 1999. Generalizing and extending the eigenshape method of shape space visualization and analysis. Paleobiology 25:107–138.

MANCHESTER, S. R. 1994. Fruits and seeds of the middle Eocene Nut Beds Flora, Clarno Formation, Oregon. Palaeontographica Americana no. 58. pp. 1–205.

MANCUSO, S. 1999. Elliptic Fourier Analysis (EFA) and Artificial Neural Networks (ANNs) for the identification of grapevine (Vitis vinifera L.) genotypes. Vitis 38:73–77.

MANOS, P. S., Z. K. ZHOU, AND C. H. CANNON. in press. Systematics of Fagaceae: phylogenetic tests of reproductive trait evolution. Int. J. Plant Sci.

MANOS, P. S., J. J. DOYLE, AND K. C. NIXON. 1999. Phylogeny, biogeography, and processes of molecular differentiation in Quercus subgenus Quercus (Fagaceae). Mol. Phylogenet. Evol. 12:333–349.

MARTINS, E. P. 1996. Phylogenies, spatial autoregression, and the comparative method: a computer simulation test. Evolution 50:1750–1765.

MCLELLAN, T. 2000. Geographic variation and plasticity of leaf shape and size in Begonia dregei and B. homonyma (Begoniaceae). Bot. J. Linnean Soc. 132:79–95.

MCLELLAN, T., AND J. A. ENDLER. 1998. The relative success of some methods for measuring and describing the shape of complex objects. Syst. Biol. 47:264.

MICKEVICH, M. F. 1982. Transformation series analysis. Syst. Zool. 31(4):461–478.

MIYAMOTO, M. M., AND W. M. FITCH. 1995. Testing species phylogenies and phylogenetic methods with congruence. Syst. Biol. 44:64–76.

MOOERS, A. O., S. M. VAMOSI, AND D. SCHLUTER. 1999. Using phylogenies to test macroevolutionary hypotheses of trait evolution in Cranes (Gruinae). Am. Nat. 154:249–259.

MOU, D., AND E. F. STOERMER. 1992. Separating *Tabellaria* (Bacillariophyceae) shape groups based on Fourier descriptors. J. Phycol. 28:386–395.

NG, F. S. P. 1991. Manual of forest fruits, seeds, and seedlings. Forest Research Institute Malaysia, Kuala Lumpur.

NIXON, K. C. 1997. Fagaceae Dumortier. Pages 436–506 *in* Flora of North America (F. o. N. A. E. Committee, ed.) Oxford University Press, New York.

PURVIS, A. 1995. A modification to Baum and Ragan's method for combining phylogenetic trees. Syst. Biol. 44:251–255.

RAGAN, M. A. 1992. Matrix representation in reconstructing phylogenetic-relationships among the eukaryotes. Biosystems 28:47–55.

RAY, T. S. 1992. Landmark Eigenshape analysis-homologous contours-leaf shape in *Syngonium* (Araceae). Am. J. Bot. 79:69–76.

RENAUD, S., J. MICHAUX, J. J. JAEGER, AND J. C. AUFFRAY. 1996. Fourier analysis applied to *Stephanomys* (Rodentia, Muridae) molars: nonprogressive evolutionary pattern in a gradual lineage. Paleobiology 22:255–265.

RICHARDS, R. A., AND C. ESTEVES. 1997. Stock-specific variation in scale morphology of Atlantic striped bass. Trans. Am. Fish. Soc. 126:908–918.

ROHLF, F. J. 1986. Relationships among Eigenshape Analysis, Fourier-Analysis, and Analysis of Coordinates. Math. Geol. 18:845–854.

ROHLF, F. J. 1990. Fitting curves to outlines. Pages 167–177 *in* Proceedings of the Michigan morphometrics workshop (F. J. Rohlf, and F. L. Bookstein, eds.). University of Michigan Museum of Zoology, Ann Arbor.

ROHLF, F. J. 1998a. tps-DIG, version 1.20. SUNY, Stony Brook.

ROHLF, F. J. 1998b. Partial warps, phylogeny, and ontogeny: a comment on Fink and Zelditch (1995). Syst. Biol. 47:168–173.

ROHLF, F. J., AND J. W. ARCHIE. 1984. A comparison of Fourier methods for the description of wing shape in mosquitoes (Diptera: Culicidae). Syst. Zool. 33:302–317.

ROHLF, F. J., AND F. L. BOOKSTEIN (eds) 1990. Proceedings of the Michigan morphometrics workshop. University of Michigan Museum of Zoology, Ann Arbor.

ROTH, I. 1977. Fruits of Angiosperms. Gebruder Borntraeger, Berlin-Stuttgart.

ROTH, V. L. 1984. On homology. Biol. J. Linn. Soc. 22:13–30.

ROTH, V. L. 1991. Homology and hierarchies: Problems solved and unresolved. J. Evol. Biol. 4:167–194.

SAKAI, S., K. MOMOSE, T. YUMOTO, T. NAGAMITSU, H. NAGAMASU, A. A. HAMID, AND T. NAKASHIZUKA. 1999. Plant reproductive phenology over four years including an episode of general flowering in a lowland dipterocarp forest, Sarawak, Malaysia. Am. J. Bot. 86:1414–1436.

SITNIKOVA, T. 1996. Bootstrap method of interior-branch test for phylogenetic trees. Mol. Biol. Evol. 13(4):605–611.

SOEPADMO, E. 1968a. Florae Malesianea precursores XLVII. Census of Malesian *Castanopsis* (Fagaceae). Reinwardtia 7:383–410.

SOEPADMO, E. 1968b. A revision of the genus *Quercus* L. *subgen*. *Cyclobalanopsis* (Oersted) Schneider in Malesia. Gard. Bull. Sing. XXII:355–427.

SOEPADMO, E. 1970. Florae Malesianae precursores XLIX. Malesian species of *Lithocarpus* BL. (Fagaceae). Reinwardtia 8:197–308.

SOEPADMO, E. 1972. Fagaceae *in* Flora Malesiana (C. G. G. J. van Steenis, ed.) Noordhoff International Publishing, Leyden, The Netherlands.

SORK, V. L. 1993. Evolutionary ecology of mast-seeding in temperate and tropical oaks (*Quercus* spp.). Vegetatio 108:133–147.

SPJUT, R. W. 1994. A systematic treatment of fruit types. Memiors of the New York Botanical Garden, v. 70. New York Botanical Garden, Bronx.

SWOFFORD, D. L., AND W. P. MADDISON. 1987. Reconstructing ancestral states under Wagner parsimony. Math. Biosci. 87:199–229.

SWOFFORD, D. L. 2001. Phylogenetic analysis using parsimony (* and other methods), version 4.0b8. Sinauer Associates.

TORRES, G. J., A. LOMBARTE, AND B. MORALES-NIN. 2000. Variability of the sulcus acusticus in the sagittal otolith of the genus *Merluccius* (Merlucciidae). Fish Res. 46:5–13.

WEBB, C. O., AND D. R. PEART. 1999. Seedling density dependence promotes coexistence of Bornean rain forest trees. Ecology 80:2006–2017.

WIENS, J. J. 1998. Testing phylogenetic methods with tree congruence: phylogenetic analysis of polymorphic morphological characters in Phrynosomatid lizards. Syst. Biol. 47:427–444.

WOLFRAM, S. 1998. The Mathematica Book, version 4.0.1. Wolfram Media/Cambridge University Press.

APPENDIX A

Taxa and specimens examined, arranged by putative section. Samples in bold were sampled for ITS sequence. All other specimens were included in the morphometric sample. Sectional names are provisional and based on A. Camus (1952–1954). Several transfers between sections have been made. New designations are based upon morphology and sequence. GenBank accession numbers are shown and the data matrix and results have been archived at TreeBase (Study #S637, Matrix #991). Collection locality abbreviations: **B**—Brunei, **SB**—Sabah, **NA**—North America, **SW**—Sarawak, **WK**—West Kalimantan, Collection numbers proceeded by SAN are part of the Sandakan Herbarium collection series. All C. H. Cannon collections are housed at Duke.

Section *Cyclobalanus*

1. *L. bennettii* (Miq.) Rehd.—**SW C.H. Cannon 67** (GenBank #AF389093), *C.H. Cannon* 632.

2. *L. blumeanus* (Korth.) Rehd.—**SW C.H. Cannon 743** (GenBank #AF389091).

3. *L. clementianus* (King ex Hook. f.) A. Camus—**SB** *C.H. Cannon* 496, *C.H. Cannon* 259: **WK** *C.H. Cannon* 596, *C.H. Cannon* 599, **C.H. Cannon 638** (GenBank #AF389107).

4. *L. encleisacarpus* (Korth.) A. Camus—**SW C.H. Cannon, Jemree, Army 70** (GenBank #AF389094).

5. *L. lucidus* (Roxb.) Rehd.—**SW C.H. Cannon, Jemree, Army 76** (GenBank #AF389088): **WK** *C.H. Cannon* 252.1.

Section *Gymnobalanus*

6. *L. havilandii* (Stapf) Barnett—**SB** ***C.H. Cannon, J.R. Harting* 506** (GenBank #AF389092).

Section *Lithocarpus*

7. *L. beccarianus* (Benth.) A. Camus—**B** *K.M. Wong* 1565 HUH: **SB** *G. Mikil* 41790 HUH: **SW** *Haji Suib* SAN23425 HUH; *C.H. Cannon* 727; *C.H. Cannon* 828: **WK** *C.H. Cannon* 612; ***C.H. Cannon* 682** (GenBank #AF389101); *C.H. Cannon* 256.

8. *L. kalkmanii* S. Julia & Soepadmo—**SB** *C.H. Cannon* 15; *C.H. Cannon* 17; ***C.H. Cannon* 24** (GenBank #AF389102); *W. Meijer* 42460 HUH.

9. *L. turbinatus* (Stapf) Forman—**SB** *C.H. Cannon* 223; ***C.H. Cannon, J.R. Harting* 510** (GenBank #AF389100); *C.H. Cannon, J.R. Harting* 513; *C.H. Cannon, J.R. Harting* 517; *C.H. Cannon, J.R. Harting* 523; *C.H. Cannon* 798; *W. Meijer* 20389 HUH; *B.E. Smythies* 10624 HUH; *C.H. Cannon* 827; *C.H. Cannon* 828: **SW** *J.A.R. Anderson* 20209 HUH.

Section *Pasania*

10. *L. conocarpus* (Oudem.) Rehd.—**EK** *F.H. Endert* 2232 HUH: **SB** *J. & M.S. Clemens* 27346 HUH: **SW** ***C.H. Cannon* 110** (GenBank #AF389095): **WK** *M.L. Leighton* 12308 DUKE.

11. *L. densiflorus* Rehd. **NA** *K. Nixon* 4585 (GenBank #AF389086) BH.

12. *L. lampadarius* (Gamble) A. Camus—**SB** ***C.H. Cannon* 88** (GenBank #AF389099): **SW** *C.H. Cannon* 766.

13. *L. luteus* Soepadmo—**SB** ***C.H. Cannon* 784** (GenBank #AF389096); *C.H. Cannon* 824.

14. *L. revolutus* Soepadmo—**SW** ***C.H. Cannon* 761** (GenBank #AF389098).

Section *Synaedrys*

15. *L. palungensis* Cannon & Manos—**SW** *C.H. Cannon* 769; ***C.H. Cannon* 768** (GenBank #AF389103).

16. *L. pulcher* (King) Markgr.—**SW** *E. Soepadmo* SAN 27607 HUH; *E.C. & L.B. Abbe* 9862 HUH; *Bojeng Sitam* 15061 HUH; *J.A.R. Anderson* 13395 HUH; *C.H. Cannon* 702: **WK** *C.H. Cannon* 652 (GenBank #AF389104).

17. *L. sericobalanus* E.F. Warb.—**SW** *B.E. Smythies* 12603 HUH; ***C.H. Cannon* 127** (GenBank #AF389105): **WK** *C.H. Cannon* 634; *C.H. Cannon* 238.

Incertae sedis

18. *L. echinifer* (Merr.) A. Camus—**SB** *M.A. Mujim* 40664 HUH; *W. Meijer* 24792 HUH: **SW** ***C.H. Cannon* 717** (GenBank #AF389089); *C.H. Cannon* 718.

19. *L. keningauensis* S. Julia & Soepadmo—**SB** *F. Sadau* 50208 HUH; *W. Meijer* 42677 HUH: **SW** ***C.H. Cannon* 751** (GenBank #AF389106).

20. *L. rotundatus* (Bl.) A. Camus—**SB** *Francis Sadau* 49504 HUH; ***C.H. Cannon* 548** (GenBank #AF389090); *C.H. Cannon* 555: **SW** *Ilias Paie* 2857 HUH.

21. *L. ruminatus* Soepadmo—**SB** *C.H. Cannon* 37; *C.H. Cannon* 47; *C.H. Cannon* 545; *C.H. Cannon* 218: **SW** ***C.H. Cannon* 113** (GenBank #AF389097); *C.H. Cannon* 116; *C.H. Cannon* 122; *C.H. Cannon* 123; *C.H. Cannon* 841: **WK** *C.H. Cannon* 255; *C.H. Cannon* 613.

Outgroups

Chrysolepis chrysophylla (Douglas ex Hooker) Hjelmquist **NA** *P. Manos* 1467 (GenBank #AF389087) DUKE.

Quercus alba L. **NA** *P. Manos* s.n. (GenBank #AF098410) BH.

Quercus acutissima Carruth. **NA** *P. Manos* s.n. (GenBank #AF098428) BH.